Molecular & Cellular Biomechanics

Tech Science Press

DOI: 10.32604/mcb.2022.018578

ARTICLE

Measurement of Myopia and Normal Human Choroidal Thickness Using Spectral Domain Optical Coherence Tomography

Jia Qin[1,2,3,4,5] and Lin An[1,2,3,4,5,*]

[1]Innovation and Entrepreneurship Teams Project of Guangdong Provincial Pearl River Talents Program Guangdong Weiren Meditech Co., Ltd., Foshan, 528000, China

[2]School of Medical Imaging, Weifang Medical University, Weifang, 261053, China

[3]School of Physics and Optoelectronic Engineering, Foshan University, Foshan, 528225, China

[4]Weiren Medical Care (Foshan) Co., Ltd., Foshan, 528200, China

[5]Weizhi Meditech (Foshan) Co., Ltd., Foshan, 528200, China

[*]Corresponding Author: Lin An. Email: weirenelex8@vip.163.com

Received: 03 August 2021 Accepted: 16 September 2021

ABSTRACT

Myopia is a common ophthalmic deficiency. The structure and function of choroid layer is assumed to be associated with myopia. In this study, a laboratory developed spectral domain optical coherence tomography scanning system is used to image human eyes. The axial resolution of the system is about 7 μm, and the acquisition rate is 100 kHz. Firstly, a cross-sectional image was acquired by averaging 100 images from imaging posterior segment of each eye. The choroid thickness was measured by 11 discrete points. The average thickness of normal human eyes was (0.296 ± 0.126) mm, whereas the average choroid thickness of myopic eyes was (0.220 ± 0.095) mm. Afterwards, the *T* test is used to calculate the data statistically. The analysis of the final result is based on the average thickness measured and the thickness of each measuring point. There was a significant difference in choroid thickness between myopia and normal eyes (*P* value < 0.01), which indicates that the choroid thickness of myopia was significantly thinner than that of normal eyes. Besides, there are findings that the choroidal thickness in nasal side is thinner than that in the fovea and temporal side in each eye. The choroidal thickness on temporal side in myopia eye has the most significant difference comparing with that in normal eye. The comprehensive evaluation of myopia and normal choroidal thickness using spectral domain optical coherence tomography may provide an important reference for the development of medical methods for diagnosis and treatment of myopia.

KEYWORDS

Spectral domain optical coherence tomography; optical image of human eyes; choroid thickness; myopia

1 Introduction

Myopia is a common ophthalmic deficiency/disease. Nowadays, as electronic equipment is more widely used, and heavy learning task of young people and other social phenomena, myopia has become a serious problem influencing the vision qualify and eye healthy.

Choroid layer is located between the retina and sclera of the human eye, which provides oxygen and nutrition for the human eye [1]. There is a large number of capillaries are distributed in the choroid. If the

capillary space of choroid is too large or the vasculature flow is insufficient, it is related to macular disease or some other diseases of human eyes. Choroid thickness, as an intuitive parameter, may have a certain correlation with myopia [2,3].

Optical coherence tomography (OCT) has been developed since 1991 [4]. From time domain to spectral domain and swept source OCT, the imaging speed, imaging resolution and signal-to-noise ratio of the system have been greatly improved. The spectral domain OCT (SD-OCT) use spectrometer to collect the coherent light information, and analyze the signals in spectral domain, which make the acquisition speed in the depth direction is much faster than that of the time domain OCT [5]. With the development of this technology, and because of the superior imaging resolution of OCT and the need of ophthalmic examination, it has been widely used in the ophthalmic examination [6,7]. SD-OCT is a noninvasive optical imaging method, which can further analyze and determine the pathogenesis of myopia by analyzing the relationship between choroid and myopia in different age groups, so that in the adolescent stage, the development of corresponding medical methods can further intervene the incidence of myopia in and children and adolescents.

In this study, the SD-OCT system is used to image the morphological structure of the fundus of human eyes, so the structure images of the choroid could be acquired and the corresponding thickness of the choroid could be evaluated.

2 Experiment

2.1 Theory of SD-OCT

Unlike other traditional imaging methods, OCT uses a low coherent light source to illuminate the imaging sample, and then obtain the depth information of the sample by the interference signal extracted from the reflected light from the sample arm and reference arm. The detected signal from the system can be expressed by the following formula (1) [8]:

$$\begin{aligned} I_D(k) &= \frac{\rho}{4}[S(k)[R_R + R_{S1} + R_{S2} + \ldots R_{Sn}]] \\ &+ \frac{\rho}{2}\left[S(k)\sum_{n=1}^{N}\sqrt{R_R R_{Sn}}(\cos[2k(Z_R - Z_{Sn})])\right] \\ &+ \frac{\rho}{4}\left[S(k)\sum_{n\neq m-1}^{N}\sqrt{R_{Sn}R_{Sm}}(\cos[2k(Z_{Sn} - Z_{Sm})])\right] \end{aligned} \tag{1}$$

In the formula (1), $I_D(k)$ is the signal collected from SD-OCT, ρ is the photoelectric conversion efficiency of the camera. $S(k)$ is the power spectrum function of the light source. R_R is the reflectivity of the reference arm. R_{Si} is the reflectivity of the sample arm. Z_R is the distance between the reference arm and the spectroscopic position. Z_{Si} is the distance between the sample and the spectroscopic position. k is the wave vector. The first term in the above formula is the DC term, which is the superposition of the reflected light intensity from the reference arm and the sample arm. The second item is the interrelated item between the returned light of the reference arm and each layer of the sample. The third term is the self-coherent term, which is the interrelated item caused by the interference between different layers' reflections of the sample arm. The imaging of OCT is mainly based on the second term, that is, the interrelated item. As shown in the above formula, with the deepening of the depth, the frequency of the signal is higher. After removing the DC term and self-coherent noise of the collected signal, the intensity information of different depths can be obtained by Fourier transform.

$$I_D(k) = \frac{\rho}{8}[\gamma(z)[R_R + R_{S1} + R_{S2} + \ldots R_{Sn}]] + \frac{\rho}{4}\left[\gamma(z) \otimes \sum_{n=1}^{N} \sqrt{R_R R_{Sn}}(\delta(Z \pm (Z_R - Z_{Sn})))\right] + \frac{\rho}{8}\left[\gamma(z) \otimes \sum_{n \neq m-1}^{N} \sqrt{R_{Sn} R_{Sm}}(\delta(Z \pm (Z_{Sn} - Z_{Sm})))\right] \quad (2)$$

The formula (2) is obtained by performing Fourier transform to the formula (1). $\gamma(z)$ is the Fourier transform of $S(k)$, $\otimes$ represents convolution. By calculating the second item in the formula, we can get the signal information of A-line scan.

The signal of a single A-line is shown in Fig. 1. Different depth positions are denoted by the abscissa, while the signal intensity of different depths of tissue is shown by the ordinate. The complete two-dimensional choroid map, shown by the OCT B-scans, can be obtained, where the choroidal thickness can be measured. The thickness of choroid is calculated from the distance between the RPE and the choroidal border. The choroidal thicknesses from multiple locations of the thickness band could be evaluated.

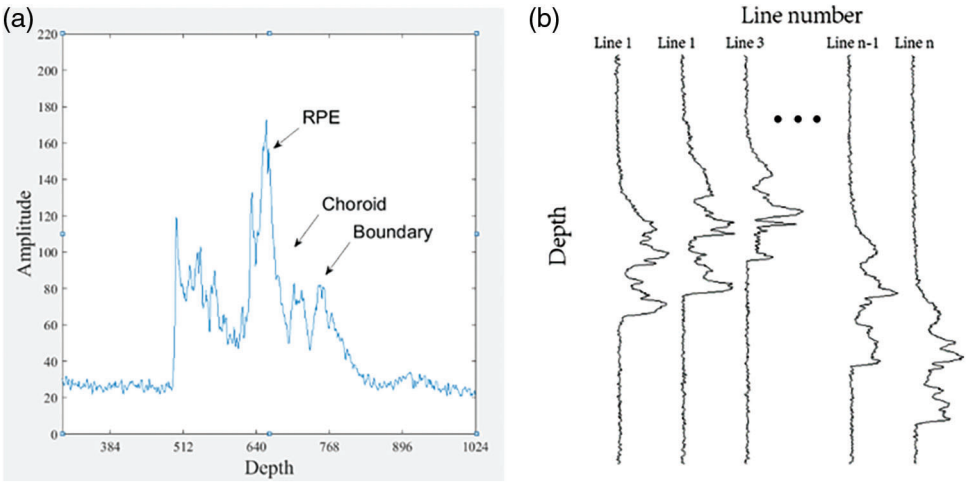

Figure 1: (a) Signal of A-line and (b) B-scans composition

The number of A-line in B-scans can be determined according to the requirements of the experiment. The imaging speed of the system can be improved by reducing the number of A-line appropriately. The number of A-line is not infinite, it is related to the lateral resolution of the system. The excessive number of A-line will cause over-sampling, which could increase the size of the data and the imaging time but not improve the quality of the image.

2.2 Experiment

Here, a SD-OCT system is used to image the fundus. The schematic and photograph of the imaging system are shown in Fig. 2.

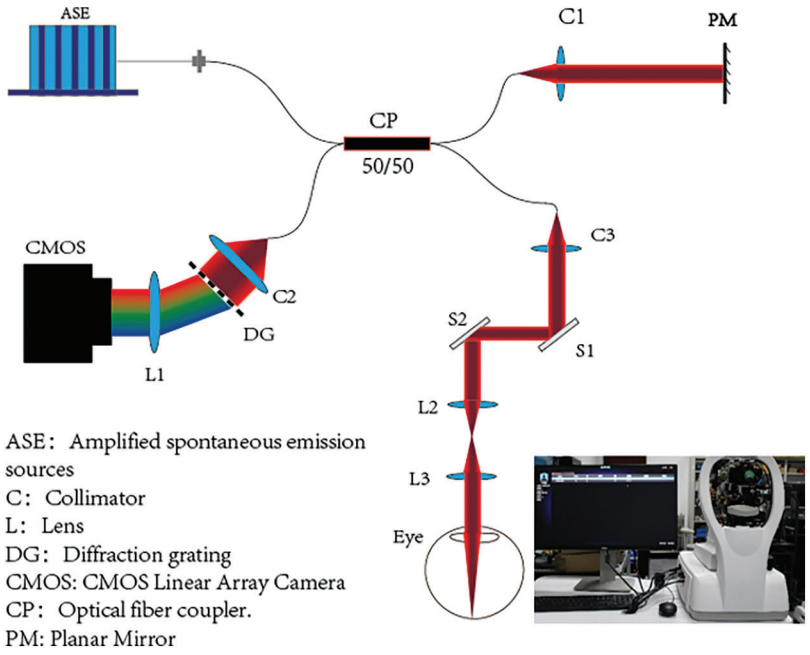

Figure 2: The structure diagram of the SD-OCT System

The initial light of the system is originated from an ASE light source (EXALOS), with a central wavelength of 840 nm and a bandwidth of 49 nm (−3 db), which is divided into two beams through an optical fiber coupler (50:50 coupling ratio, Thorlabs). One beam of the light enters the reference arm through the collimator (Thorlabs); the other beam of the light enters the sample arm through the optical fiber collimator, and then controls the tomography imaging position of the system through an X-Y scanning galvo mirror systems (Thorlabs). Finally, it passes through the objective lens group composed of L2 and L3, and then focuses on the retina and choroid area through the optical system of the eye. The reflected light from the reference arm and the backscattered light from the sample arm go into the imaging acquisition section after being coupled into the optical fiber couplers. The returned light passes through a collimated lens (focal length is 75 mm) and then hits on the grating (1800 L/mm, Wasatch). Then, through a focusing lens (focal length is 150 mm), the signal is collected on the photosensitive layer of the camera (E2V). The fastest imaging speed of the camera is 140 K. The imaging speed of the system is 100 kHz. The axial resolution of the system is about 7 μm. The measurement sample of this experiment is human eye fundus. Setting the average refractive index of its tissue to be 1.375. The power of the irradiated light at the pupil is about 2 mW, which meets the requirements of GB7247 and ISO-15004.

There were 10 volunteers in this experiment. The purpose and significance of the study have been informed to the subjects with agreements. In the 10 subjects, four of them have normal eyes and were used as control group A. Six of them have myopic eyes, which were used as experimental group B. Through imaging 20 eyes of the 10 subjects at the same specified period on different dates, clear choroid fundus images were obtained, and an average of 11 points of choroid were measured. Finally, the data sets were analyzed and compared.

The image acquisition speed by the system is set to 100 kHz. Each picture consists of 1000 A-line, that is, the size of the picture is 1024 pixels × 1000 pixels, and the frame rate is 100 Hz. A total of 100 pictures were collected per collection, the acquisition time is 1 s. Then, 100 pictures were averaged, and a representative image was obtained in Fig. 3. As to the measurement of the choroid thickness, 11 measuring points were selected, including the measuring point 5 showing in the fovea region,

4 measuring points on the left (nasal) side of the central fovea, and 6 measuring points on the right (temporal) side of the central fovea. The measuring points of each picture were consistent with the same location and intervals.

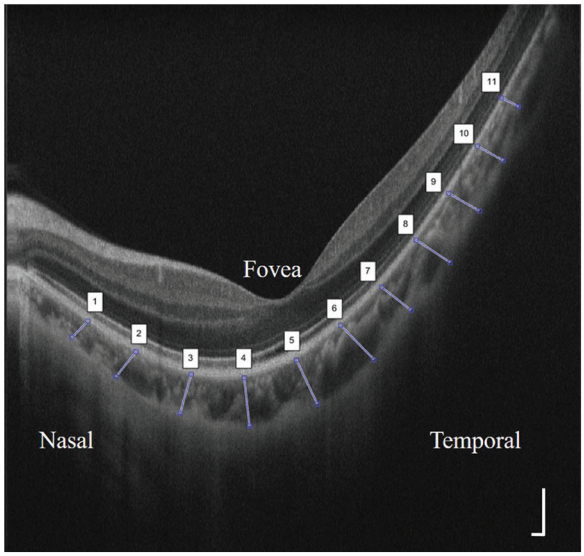

Figure 3: Demonstration of fundus cross-sectional map and measurement positions of different choroid thicknesses. Left: nasal side; right: temporal side. Scale bar is 200 μm

3 Analysis and Discussion

The collected data, incorporating average value, positive and negative deviation, were analyzed by SISS 25 software. The t test was implemented to the measured data independently, and $P < 0.05$ difference denotes statistically significant. The results were shown in Table 1 & Fig. 4. According to Table 1, the thickest region of choroid was in the temporal side, followed by the central fovea thickness. The nasal side was the thinnest, which was consistent with the previous study [9]. As shown in Table 1, the average measurement result of the choroid thickness in normal human eyes was 0.296 (±0.126) mm. The average choroid thickness of myopic eyes was (0.220 ± 0.095) mm. The T value of T test was 20.262, $P < 0.01$, that is to say, the choroid thickness of myopia group was significantly different from that of normal human eyes. Moreover, there were significant differences at each measuring point, which indicated that the choroid thickness of myopic eyes became thinner than that of normal eyes. The choroidal thickness on temporal side in myopia eye has the most significant difference comparing with that in normal eye.

Table 1: Measurement and evaluation of the choroidal thickness in normal and myopia eyes

Choroidal thickness	Normal (mm)	Myopia (mm)	T	*P* value
Average thickness	0.296 ± 0.126	0.220 ± 0.095	20.262	<0.01
Nasal thickness	0.2327	0.17787	9.731	<0.05
Temporal thickness	0.3313	0.2514	23.631	<0.01
point 1	0.170 ± 0.110	0.126 ± 0.059	11.496	<0.01
point 2	0.211 ± 0.122	0.149 ± 0.070	13.140	<0.01

(Continued)

Table 1 (continued)

Choroidal thickness	Normal (mm)	Myopia (mm)	T	*P* value
point 3	0.251 ± 0.116	0.176 ± 0.073	14.355	<0.01
point 4	0.299 ± 0.108	0.218 ± 0.118	16.042	<0.01
point 5	0.341 ± 0.078	0.248 ± 0.134	17.007	<0.01
point 6	0.366 ± 0.065	0.275 ± 0.114	19.251	<0.01
point 7	0.371 ± 0.066	0.277 ± 0.093	22.599	<0.01
point 8	0.356 ± 0.086	0.270 ± 0.086	22.817	<0.01
point 9	0.325 ± 0.069	0.247 ± 0.089	21.685	<0.01
point 10	0.302 ± 0.063	0.228 ± 0.075	20.343	<0.01
point 11	0.269 ± 0.062	0.211 ± 0.079	22.141	<0.01

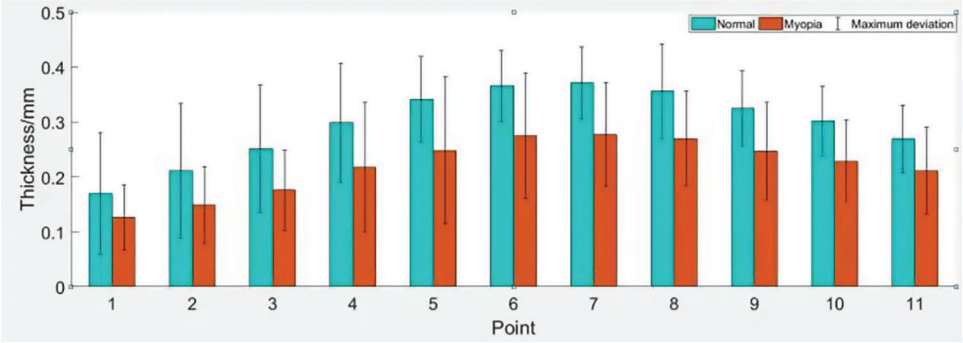

Figure 4: The schematic diagram of the measured results. Choroidal thickness values in normal eyes are denoted by the blue bars. Choroidal thickness values in myopia eyes are denoted by the orange bars

4 Conclusion

Overall, a comprehensive evaluation of myopia and normal choroidal thickness using spectral domain optical coherence tomography is reported here. The choroid thickness of myopia was significantly thinner than that of normal eyes (P value < 0.01). The choroidal thickness on temporal side in myopia eye has the most significant difference by comparing with that in normal eye. Besides, the choroid thickness values in temporal, fovea and nasal areas become thinner gradually. The study may provide an important reference for the development of therapeutic strategies for myopia.

5 Discussion

The thickness of choroid is negatively correlated with the degree of myopia, that is, the thinner the choroid is, the deeper the degree of myopia. In the future, three dimensional imaging of the choroid morphological structure and the choroid blood vessels will be compared and analyzed with the degree of myopia. Relationship between myopia and the volumetric structure and function of the choroid will be investigated.

Acknowledgement: We thank the support from the research lab in Guangdong Weiren Meditech Co., Ltd. and Foshan University.

Funding Statement: Guangdong Provincial Pearl River Talents Program (2019ZT08Y105). Foshan HKUST Projects (FSUST21-HKUST10E). National Natural Science Foundation of China (81771883). National Natural Science Foundation of China (81801746). Thousand Young Talents Program of China (IQ2025). Guangdong University Scientific and technological achievements transformation University Characteristics Innovation Research Project (2019XJZZ01). Guangdong–Hong Kong–Macao Intelligent Micro-Nano Optoelectronic Technology Joint Laboratory (2020B1212030010).

Conflicts of Interest: The authors declare that they have no conflicts of interest to report regarding the present study.

References

1. Nickla, D. L., Wallman, J. (2010). The multifunctional choroid. *Progress in Retinal & Eye Research, 29(2),* 144–168.
2. Ohno-Matsui, K., Lai, T. Y. Y., Lai, C. C., Cheung, C. (2016). Updates of pathologic myopia. *Progress in Retinal & Eye Research, 52,* 156–187.
3. Ignacio, F. M., Francisco, L., Duker, J. S., Ruiz-Moreno, J. M. (2013). The relationship between axial length and choroidal thickness in eyes with high myopia. *American Journal of Ophthalmology, 155(2),* 314–319.e1.
4. Huang, D., Swanson, E. A., Lin, C. P., Schuman, J. S., Stinson, W. G. et al. (1991). Optical coherence tomography. *Science, 254(5035),* 1178–1181.
5. Velthoven, M., Faber, D. J., Verbraak, F. D., Leeuwen, T., Smet, M. (2007). Recent developments in optical coherence tomography for imaging the retina. *Progress in Retinal & Eye Research, 26(1),* 57–77. DOI 10.1016/j.preteyeres.2006.10.002.
6. Mrejen, S., Spaide, R. F. (2013). Optical coherence tomography: Imaging of the choroid and beyond. *Survey of Ophthalmology, 58(5),* 387–429. DOI 10.1016/j.survophthal.2012.12.001.
7. Ravi, T. (2018). Anterior segment optical coherence tomography. *Progress in Retinal & Eye Research, 25(5–6),* 317–323.
8. Izatt, J. A., Choma, M. A. (2008). Theory of optical coherence tomography. In: Drexler, W., Fujimoto, J. G. (Eds.), *Optical coherence tomography,* pp. 47–72. Berlin, Heidelberg: Springer.
9. Elise, H., Leslie, H., Jane, G., Wendy, M. T., Zhang, Q. H. et al. (2015). Choroidal thickness profiles in myopic eyes of young adults in the correction of myopia evaluation trial cohort. *American Journal of Ophthalmology, 160(1),* 62–71.E2. DOI 10.1016/j.ajo.2015.04.018.